River sediment geochemistry as a conservative mixture of source regions: Observations and predictions from the Cairngorms, UK

Alex G. Lipp[1*], **Gareth G. Roberts**[1], **Alexander C. Whittaker**[1], **Charles. J. B. Gowing**[2], **and Victoria M. Fernandes**[1]

[1]Department of Earth Sciences and Engineering, Imperial College London, UK
[2]Centre for Environmental Geochemistry, British Geological Survey, Keyworth, UK

Abstract

The elemental composition of sediments in rivers is the product of physical and chemical erosion of rocks, which is then transported across drainage networks. A corollary is that fluvial sedimentary geochemistry can be used to understand geologic, climatic and geomorphic processes. We develop a simple methodology to predict elemental compositions of river sediments from digital elevation data and geochemical maps using erosional models. We test these models using a new sedimentary geochemical dataset from carefully chosen sample sites. Sediment compositions are predicted by formally integrating eroding substrates with known compositions across drainage basins. Different parameterisations of erosional models, including the Stream Power formulation and uniform incision rates, are tested. Substrate chemistry was determined from the G-BASE geochemical survey. Predictions are tested using a new suite of compositions obtained from fine grained ($< 150\,\mu$m) sediments at 67 sites along the Spey, Dee, Don, Deveron and Tay rivers, Cairngorms, UK. Results show that sedimentary geochemistry can be predicted using simple models that include the topography of drainage networks and substrate compositions as input. Our predictions in this location are insensitive to the choice of erosional model, which we suggest is a consequence of broadly homogeneous rates of erosion throughout the study area. Principal component analysis of the river geochemical data suggests that the composition of most Cairngorms river sediments can be explained by mafic/felsic provenance and conservative mixing downstream. Successful prediction of sedimentary geochemistry suggests that inverting the composition of ancient sedimentary rock might allow quantitative reconstruction of specific past environmental conditions.

Plain Language Summary

The chemistry of sediments in rivers is used to understand many geologic, climatic and biotic processes including climate change and mountain building. For example, geochemical data acquired along rivers have been used to constrain rates of CO_2 drawdown. Acquiring observations of river chemistry and testing their sensitivity to physical and chemical processes (e.g. tectonics, weathering, climate) is generally challenging. Therefore, developing methods to predict the composition of river sediments from first principles, or from readily available data, is attractive. We address this problem by combining maps of geochemical data with models of erosion to predict the composition of river sediments. These predictions are tested using new observations from the Spey, Dee, Don, Deveron and Tay rivers, which drain the Cairngorms mountains, UK. The model predictions are mostly correct. Results suggest that the chemistry of river sediments are primarily mixtures of the composition of source regions. Physical erosion and the shape and connectivity of drainage basins controls the chemistry of river sediments downstream, other processes (e.g. storage) appear to play secondary, moderating, roles. In the Cairngorms, we find that most river sediment geochemistry can be related to mixing of just two types of igneous rock (mafic and felsic).

1 Introduction

The elemental composition of river sediments is determined by the chemistry of the eroding substrate (e.g. bedrock, soils) and modified by processes including chemical weathering, cation exchange and hydrodynamic sorting (e.g. Bouchez et al. 2011, 2012; Lupker et al. 2016). Consequently, river sediment compositions are used to investigate controls on chemical and physical weathering rates (e.g. climate change, tectonics, geomorphic processes; Gaillardet et al. 1999; Riebe et al. 2003; Blanckenburg et al. 2012). Geochemical studies of fluvial sediment commonly make use of samples along rivers to qualitatively infer climatic or erosional processes upstream. In such studies, assumptions about how the upstream signal is integrated downstream are common, e.g. 'let nature do the averaging' (Blanckenburg 2005; Weltje 2012; Romans et al. 2016; Garzanti et al. 2018 and references therein). Studies of this type represent a step towards making use of fluvial sedimentary signals preserved in the geological record to constrain surface processes on geological timescales.

The central aim of this study is to develop and test methodologies that can predict the composition of river sediments at any position in a drainage basin. Whilst geostatistical approaches to interpolate geochemical data along stream networks have been proposed (e.g. Kim et al. 2017), we instead take a deterministic modelling approach incorporating quantitative, objective, evaluation of assumptions about how physical and chemical

*correspondence: a.lipp18@imperial.ac.uk

signals propagate through fluvial systems. The ultimate aim is to accurately predict sediment compositions at river mouths where sediments are transferred to the marine realm and can be preserved as stratigraphy. The forward models developed in this study are a step towards inverting stratigraphic records for histories of physical and chemical surface processes (see Straub et al. 2020).

Modelling of surface processes has become increasingly tractable due to the availability of high resolution topographic data and computationally efficient landscape evolution models (e.g. Braun et al. 2013; Hobley et al. 2017; Salles et al. 2018; Salles 2019). These advancements have made it possible to make testable predictions about a range of observable characteristics such as exhumation rate and fluvial sedimentary flux (e.g. Fernandes et al. 2019).

Recently, landscape evolution models have been modified to make theoretical predictions about sediment provenance (e.g. Sharman et al. 2019). Predictions from such models could be tested using, for example, geochemical observations. Making testable predictions of sediment chemistry along drainage networks requires information of the chemistry in the source regions. It remains unclear at what density the source region must be physically sampled to make accurate predictions of downstream sediment compositions. We therefore start by making use of high resolution regional geochemical surveys, generally produced for environmental monitoring and mineral exploration purposes Garrett et al. 2008. These inventories can span large regions and contain samples acquired at regular intervals with a consistent methodology, which make them ideal for our purposes (e.g. Smith et al. 2013; Caritat et al. 2016).

In this study we make use of the high resolution Geochemical Baseline Survey of the Environment (G-BASE), UK, combined with a new complementary dataset of higher-order river sediment geochemistry gathered specifically for this study (Johnson et al. 2005). The G-BASE survey produced elemental chemistry of sediment samples acquired principally from low-order streams across the UK. The G-BASE survey is distinguished from other geochemical surveys by its high spatial sampling density. G-BASE samples the UK with an average density of 1 site per 2 km^2. We note that other large scale base-line surveys exist but often at lower densities, for example, the National Geochemical Survey of Australia samples at a density of 1 site per 5,500 km^2.

Model predictions are tested using a new inventory of 67 samples acquired for this study along higher-order rivers draining eastern Scotland, UK. We focus on the Spey, Tay, Dee, Don and Deveron rivers, which drain the Cairngorms massif and surrounding region of northeastern Scotland, UK (Figure 1). This region contains some of the highest topography in the UK. It also contains significantly variable geological units (Figure 1b). For example, the Cairngorms massif contains Paleozoic granites and mafic rocks intruded into sedimentary and metasedimentary rocks. The diverse array of lithologies, combined with high natural sediment supply provides an opportunity to explore the roles that substrate geochemistry and erosional processes play in determining fluvial sediment geochemistry.

2 METHODS

2.1 Predicting sediment geochemistry

The downstream composition of river sediment can be predicted using information about the properties of eroding substrate (e.g. elemental composition of lithologies) and incision rates, $\partial z/\partial t$ (where z is elevation and t is time). The latter can be estimated using geologic or geomorphic observations and from topographic data. First, consider some spatially variable and measurable geochemical characteristic of sediment, C (e.g. wt% MgO, where wt% = weight percent). By assuming instantaneous transport of eroded sediment, the composition of river sediments C_{sed} along a river of length L is given by

$$C_{sed} = \frac{1}{\int_x^L \frac{\partial z}{\partial t}(x)\mathrm{d}x} \int_x^L \frac{\partial z}{\partial t}(x)C(x)\mathrm{d}x. \qquad (1)$$

This expression calculates the contribution of source regions to the value of C_{sed} —by integrating the product of composition and incision rate with respect to distance downstream between positions x and L. Importantly, the contribution of elements from each eroding patch of the landscape are normalised by total sedimentary flux.

A suite of observational and theoretical approaches exist to calculate incision rates and sedimentary fluxes at a range of spatial and temporal scales (e.g. Syvitski et al. 2007; Holbrook et al. 2014; Stephenson et al. 2014). For example, cosmogenic dating of fluvial terraces and erosion of radiometrically dated basalt flows constrain incision rates at spot locations on time scales of 1 kyr to 1 Myr (e.g. Karlstrom et al. 2008; Stucky de Quay et al. 2019). Erosional models are also frequently used to calculate incision rates continuously across a landscape.

We first examine predictions from the widely used Stream Power erosional model, which relates incision rates to discharge and slope, $\partial z/\partial x$, through a power law relationship (e.g. Howard et al. 1983; Rosenbloom et al. 1994; Tucker et al. 2002). This model for fluvial erosion is simple, widely applied in a range of different environments and can be readily extended to consider other factors such as 'diffusive' geomorphic processes. It represents therefore a reasonable starting point for predictive modelling of fluvial sedimentary geochemistry. Using upstream drainage area, $A(x)$, as a proxy for river discharge results in the following Stream Power formulation of fluvial incision rate along rivers

$$\frac{\partial z}{\partial t} = -vA(x)^m\left(\frac{\partial z}{\partial x}\right)^n, \qquad (2)$$

where v, m, and n are independent parameters that can be calibrated using the topology of drainage networks and independent geologic data. This formulation is often presented as $E(x,t) = -vA^mS^n$, where S is slope and E is erosion rate. The Stream Power model can be generalised to two spatial dimensions (e.g. x and y), such that, when $n = 1$,

$$\frac{\partial z}{\partial t} = -vA^m\nabla z. \qquad (3)$$

The composition of eroded and transported sediment can therefore be predicted throughout a landscape by combining Equa-
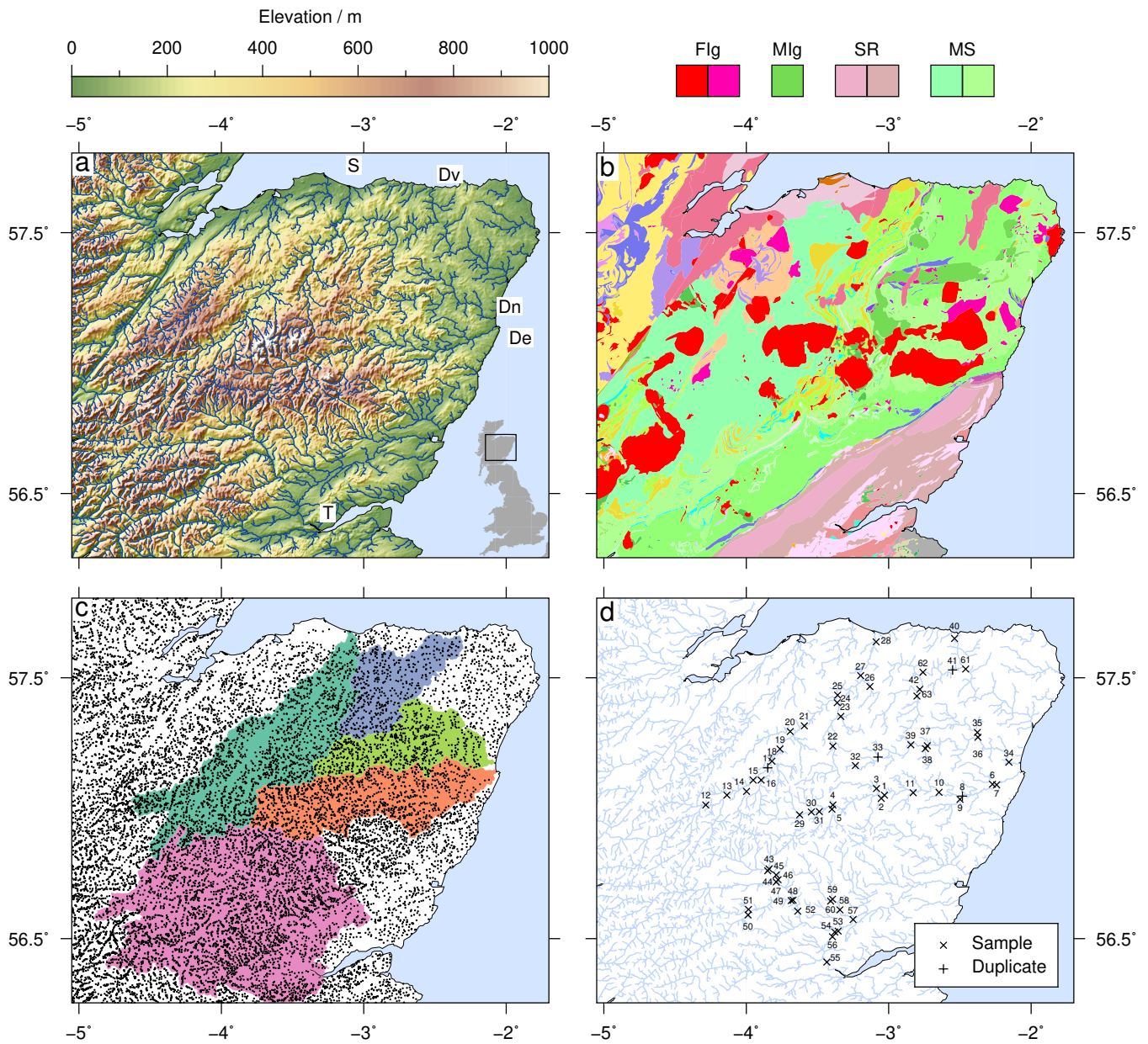
Figure 1: **Introduction to studied region: Scotland, UK.** (a) Topography from SRTM1s data set gridded to 200×200 m squares. Blue = rivers from CCM2 database (Jager et al. 2010). Rivers labelled: S = Spey, Dv = Deveron, Dn = Don, De = Dee, T = Tay. Inset map shows locality of study region within the rest of UK. (b) Geological map showing key lithologies: Flg = Ordovician to Devonian felsic igneous intrusions; Mlg = Ordovician to Silurian mafic igneous intrusions; SR = Sedimentary rocks, mostly Devonian sandstones; MS = Metasedimentary rocks, mostly Neoproterozoic psammites. See mapapps.bgs.ac.uk/geologyofbritain/home.html for full geologic key; reproduced with the permission of the British Geological Survey UKRI, all rights reserved. (c) Black circles = G-BASE sample localities overlain on river catchments. (d) Symbols × and + indicate localities where single and duplicate samples were acquired, respectively. Numbers = localities.

tions 1 and 3. We make use of topographic data, $z(x, y)$, and continuous maps of source region geochemistry, $C(x, y)$, to parameterise these equations. We start by assuming spatially constant erosional parameter values to predict incision and flux (Figure 2a-d). Initially we use the linear form of the Stream Power model as it is tractable and has been applied successfully on both small scale and regional scales. For example, inversions of large inventories of river profiles have found that $n \simeq 1$ and $0.2 \leq m \leq 0.7$ produce theoretical river profiles that best fit observed longitudinal river profiles in continents including Eurasia, North and South America, Africa and Australia (e.g. Paul et al. 2014; Fernandes et al. 2019). Therefore, we start by setting $n = 1$ and $m = 0.35$. We acknowledge that a range of different values of m and n are preferred and systematically test the effect of changing these parameter values for our results (see Whipple et al. 2002 and references therein). The parameter v is often interpreted as representing bedrock erodibility. For this study, v is assumed to be constant across the region, meaning that the predicted composition of sediment (Equation 1) is independent of the specific value of v.

Equations 1 and 3 are implemented using the LandLab package in python 3 (Van Rossum et al. 2009; Hobley et al. 2017). The SRTM1s topographic dataset was gridded to 200×200 m squares following a cylindrical equal-area projection centred on our study area using GMT 5.4.5 (Farr et al. 2007; Wessel et al. 2013). Depressions in the topography were filled using the 'priority-flood' algorithm and flow directions are computed using the 'D8' algorithm (Barnes et al. 2014). Code to reproduce our implementations of Equations 1 and 3 are provided (see Acknowledgements for access details).

2.2 Source region chemistry: G-BASE inventory

Maps of source region geochemistry were generated using the G-BASE stream sediment survey, courtesy the British Geological Survey (BGS; Johnson et al. 2005). The G-BASE survey sampled the fine ($< 150 \, \mu$m) fraction of bedload sediments in first and second order streams across the UK; sample density is ~ 2 km^2 in our study area. A broad suite of elements were measurement from each sample. For most elements within our study region Direct Reading Optical Emission Spectroscopy was used for the analysis. Delayed Neutron Activation was used to measure Uranium. Details of the G-BASE sampling, analytical and quality control procedures are given by Johnson et al. (2018a,b). The G-BASE sample sites for our study area are shown in Figure 1c.

The concentration of most elements in the G-BASE dataset has a log-normal distribution. Therefore, to generate continuous maps of elements we interpolated the $\log_{10}$ transform of the wt% of each element. The interpolated grids have a resolution of 200×200 m (Figure 2e,f). The observations were interpolated using the continuous curvature splines methodology of Smith et al. (1990) with tension factor of 0.25. Varying the tension factor between 0 and 1 made negligible difference to predictions.

2.3 Higher order river sediment sampling and analysis

2.3.1 Sampling

The G-BASE dataset does not contain samples from higher order rivers. To evaluate our model we therefore sampled fine grained

sediments along the Spey, Tay, Dee, Don and Deveron rivers in August 2019. 67 sample sites were chosen to include uppermost reaches of the rivers, major tributaries, downstream of tributary outlets and close to the river mouths (Figure 1d). To maintain consistency between the model input data and our test dataset, the sampling procedure was identical to the original G-BASE approach and used the same equipment (Figure 3a).

Bedload sediment was extracted by shovel from the active channel of the river. Examples of sample sites are shown in Figure 3b-d. For practical reasons we focused on deposits near to the bank (e.g. Figure 3c,d). If multiple shovel loads were required, as much as was possible, they were extracted from the same point in the channel bottom. The extracted sediment was first shaken through a 2 cm metal grill to remove pebbles. Subsequently, the wet sediment was deposited on a sieve stack on top of a fiberglass collecting pan. Using rubber gloves the sediment was rubbed through a 2 mm nylon mesh and washed through with a small amount of river water. This upper mesh was removed and the < 2 mm sediment fraction was then rubbed and washed through a 0.15 mm nylon mesh into the collecting pan beneath. This procedure was repeated until ~ 100 g of sediment had collected in the pan. The collecting pan was left undisturbed and covered for 20 minutes to allow sediment to fall out of suspension. Excess water, which contained some very fine sediment in suspension, was carefully decanted leaving a slurry of sediment behind. This slurry was homogenised and poured through a funnel into a labelled reinforced paper sample bag. Any sediment residue was then washed into the sample bag with a small amount of water. The bag was sealed and placed in a sealed plastic bag. A video showing the sampling procedure can be found in the Supporting Information.

To limit cross-contamination, the sampling kit was washed in river water, downstream of the site, before and after sampling. Sample numbers were pre-allocated in a randomised order. For example, localities 1, 2 and 3 had pre-allocated sample numbers CG020, CG062 and CG044 respectively. This randomisation was performed to avoid systematic bias during preparation and analysis, when samples were handled in numeric order (Johnson et al. 2018a). At the end of each field day samples were dried in paper bags until they had the consistency of modelling clay. Special care was taken to avoid contaminating samples at this stage. The dried sediments were then placed into polyester bags and sealed again. After the sampling was concluded, samples were freeze-dried for storage before analysis.

2.3.2 Geochemical Analysis

The freeze dried samples were disaggregated with a rubber mallet and homogenised by cone-quartering. 20 g of the homogenized sample were then powderised in an agate ball mill. ~ 0.25 g of powder were weighed into Savillex tubes for digestion. The samples were pre-digested in HNO$_3$ to remove organic compounds. Subsequently the samples underwent hotplate mixed acid (HF, HNO$_3$ and HClO$_4$) digestion over a ramped heating procedure. After digestion the samples were resolubilised in aqueous HNO$_3$ and H$_2$O$_2$. The liquid samples were then analysed for a full suite of elements by Inductively Coupled Plasma Mass Spectrometry. Comparison to external and internal standards indicates that some elements (particularly Zr and Hf) were only partially digested suggesting a residue of particularly chemically resistant minerals such as Zircon. The majority of other
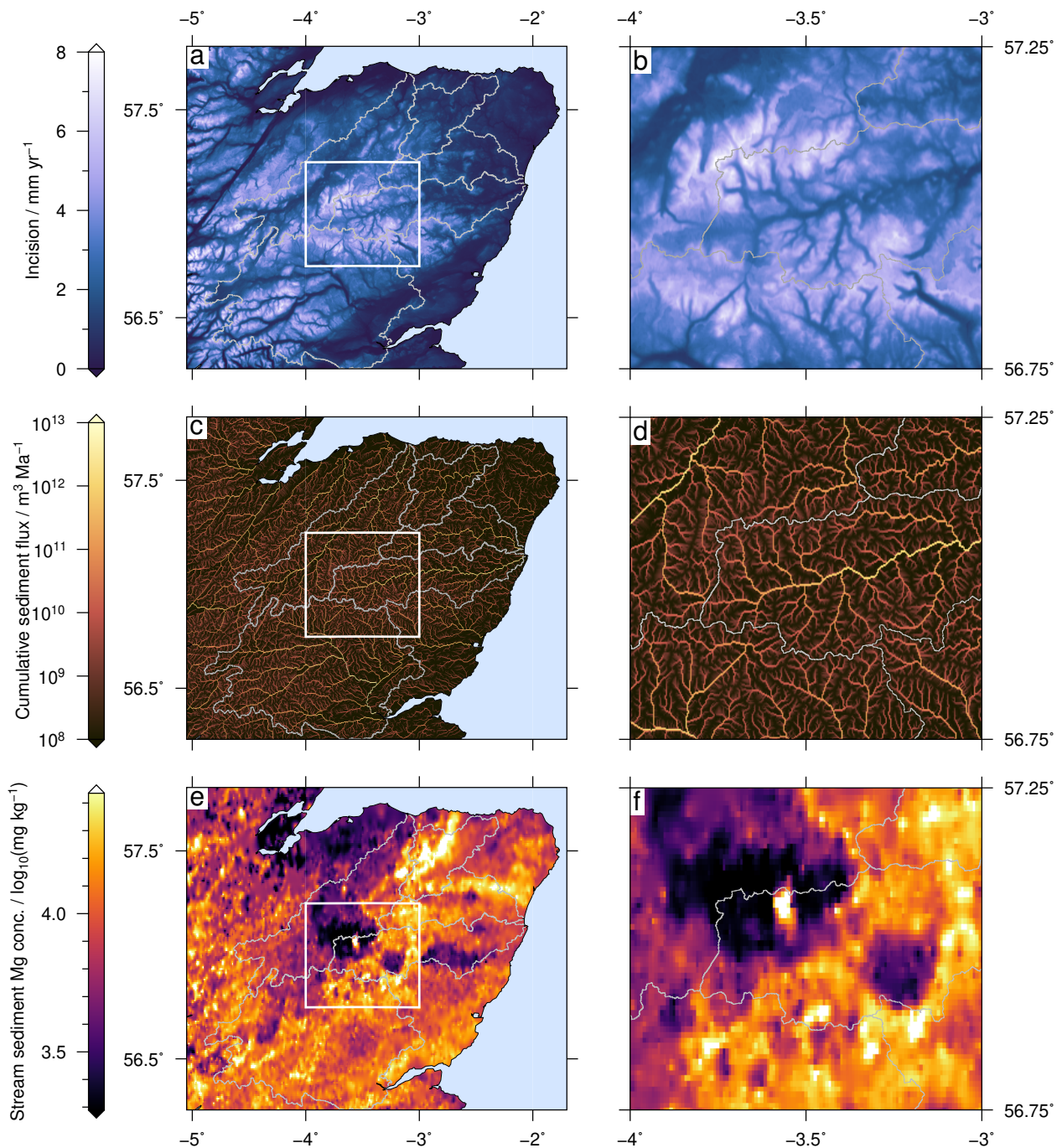
Figure 2: **Inputs used in geochemical predictions.** (a) Predicted incision, calculated using SRTM data set (Figure 1a) and Equation 3 with $n = 1$, $m = 0.35$, $v = 3.62$ m$^{0.3}$ Ma^{-1}. (b) White box = panel (b), which shows upper portion of Dee catchment. Grey lines indicate catchment boundaries. (c–d) Predicted cumulative sediment flux calculated by integrating incision (panel a) along flow paths. (e–f) Mg composition of first order stream sediments interpolated from G-BASE localities using a continuous curvature spline with a tension factor of 0.25 (Figure 1c). Analogous maps were generated for all elements.
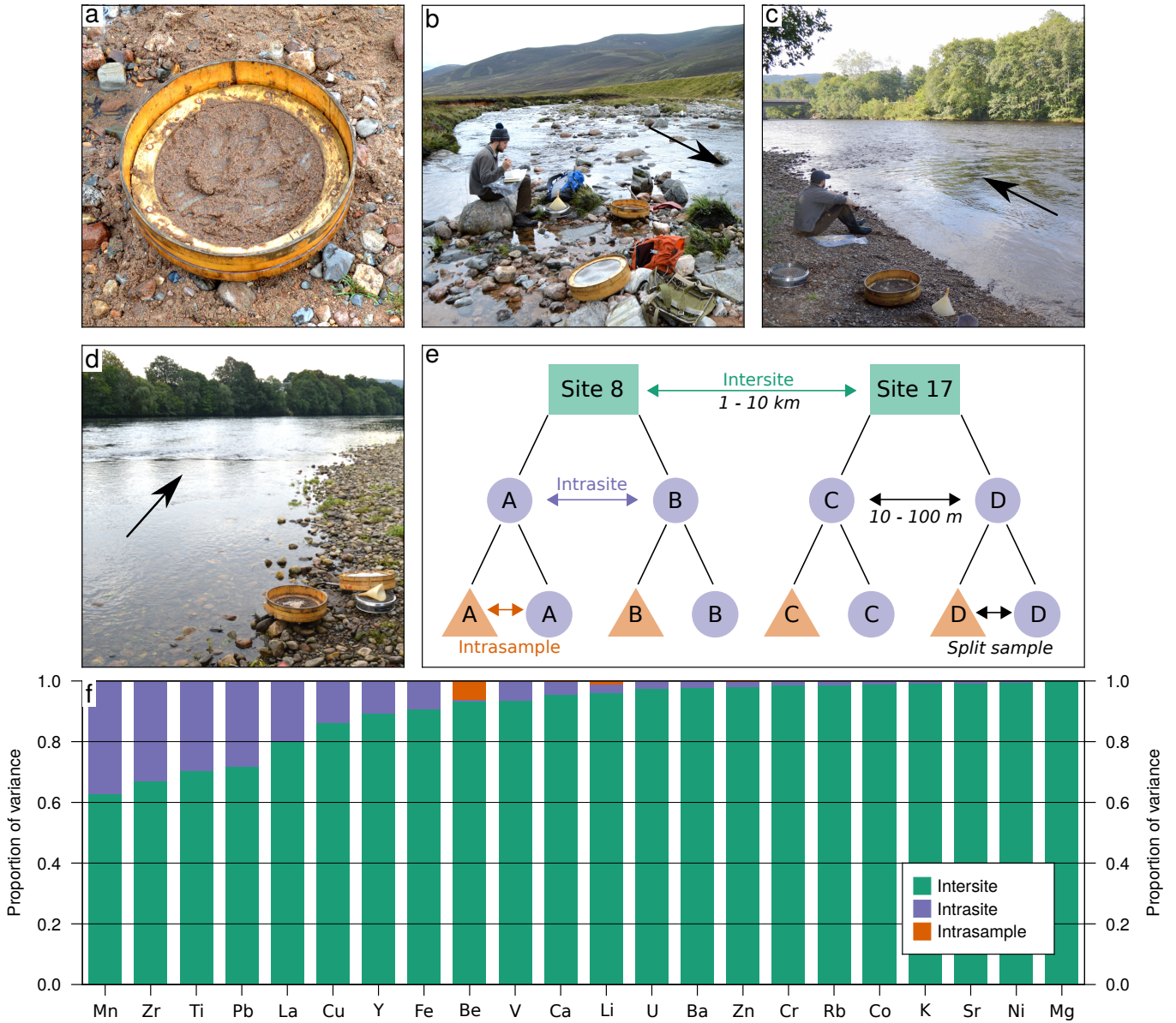
Figure 3: **Sampling methodology and analysis of variance (ANOVA).** (a) Nested sieve set used for sampling. Photograph shows sediment on top of 150 μm mesh atop collecting pan; apparatus has a 45 cm diameter. (b) Photograph shows Locality 29 (upper reaches of River Dee); arrow indicates flow direction. (c) Locality 48, River Tummel, a tributary of Tay. (d) Locality 55, close to mouth of River Tay at Perth. (e) Schematic of nested sampling procedure. Coloured text under Site 8 indicates the hierarchy of variance (see panel f). Black text under Site 17 indicates how sample hierarchy was created. (f) Results of nested ANOVA indicates that most variance lies between sites for all studied elements, thus large scale geochemical signals dominate over local heterogeneity. Intrasample variance is negligible in most cases.

elements in the standards were successfully reproduced. All sample preparation and analysis was carried out at the BGS Inorganic Geochemistry Facility in Keyworth, UK.

For the remainder of this study we focus on the following 22 elements, which were consistently recorded in the G-BASE inventory: Ba, Be, Ca, Co, Cr, Cu, Fe, K, La, Li, Mg, Mn, Ni, Pb, Rb, Sr, Ti, U, V, Y, Zn and Zr. The new data set of chemistry for higher-order rivers is provided (see Acknowledgements for access details).

2.3.3 Nested duplicate and replicate analysis

The goal of our study is to identify and predict geochemical differences between sample sites, i.e. intersite variability. These intersite differences may however be obfuscated if there is geochemical heterogeneity within each sample site, or introduced by our analytic procedure. To investigate the ability of our procedure to identify regional geochemical signals we conducted a nested sampling procedure (Figure 3e). Nested sampling procedures are commonly used in geochemical surveying to quantify the amount of intersite, intrasite and intrasample variability and hence evaluate the success of the sampling and analytical procedure.

We implemented this nested procedure by gathering duplicate samples at four randomly chosen localities (Figure 1d). The duplicate samples were gathered exactly as described above but at a distance of ~ 100 m from the previous sampling point. Prior to powderisation, each homogenised duplicate sample was then split into two 'replicate' samples to investigate intrasample variability such that each duplicated site yields four analyses (Figure 3e).

We use a nested Analysis of Variance (ANOVA) to quantify the intersite, intrasite and intrasample variance for each of the studied elements in the 16 replicate/duplicate samples (Garrett 1969). Nested ANOVA partitions an element's variance (the spread of values for a given element, given by σ^2) into specified hierarchies (e.g. Figure 3e). In doing so it reveals the contribution from intersite, intrasite and intrasample variability towards an element's variance. Because the elements had a log-normal distribution we perform ANOVA on each element after applying a $\log_{10}$ transform. The proportion of variance in each hierarchy is shown in Figure 3f. The intersite variance accounts for > 90 % the total variability for most elements. This indicates that regional geochemical signals dominate over local variability. In most instances, the intrasample variance, which mostly reflects measurement uncertainty in our analytical procedure, is negligible. For Be, the relatively high intrasample variance is also reflected in the digestion repeats where Be shows variability between the repeats. Given that the intrasample variability is so small for all elements we use the arithmetic mean of the two replicates to represent the duplicate value for subsequent analyses. We conclude that our sampling and analytical methodology is successful in identifying meaningful regional geochemical signals between sample sites.

3 RESULTS

Figure 4a shows observed sediment Mg concentrations and model predictions. Figures 5 and 6 show results for elements that are well and poorly matched by predictions. Results for all other elements are displayed in Figures S1 and S2 of the Supporting Information.

The model predictions show significant variability in sediment geochemistry, even within relatively small areas. For example, the Don has a higher theoretical Mg concentration at its mouth than the Dee, despite being separated by only ~ 4 km (Figure 4). River chemistry is predicted to evolve along river channels. The Dee, for example, has very low predicted concentrations of Mg in its upper reaches but sediment becomes progressively more enriched in Mg towards its mouth. Variability on this scale can be observed in the predictions for all elements. Visual inspection of maps showing observed and theoretical sediment chemistry indicates that our simple model, which incorporates substrate chemistry and drainage networks, can reliably predict river sediment chemistry for many elements.

We formally compare the observed and predicted elemental concentrations by calculating Root Mean Square (RMS) misfit and R^2 values. These statistics are calculated using the $\log_{10}$ transformed data for two reasons. First, the data has a log-normal distribution, and secondly, if raw data (wt%) was used, strong heteroscedasticity was observed, which violates the underlying assumptions of the chosen statistics. To extract model predictions for each observation we select the closest model cell that exists in a channel (defined as a cell with upstream area > 25 km²). This procedure was checked manually for each locality. These statistics are given for every element alongside the results maps (Figures 4, 5, 6, S1, S2).

The misfit is calculated as the difference between the (log transformed) predicted and observed values, i.e. $x_{obs} - x_{pred}$. In most instances the misfits of the elements are distributed around 0 indicating limited bias. Ca is an example of an exception in that it appears consistently under-predicted by our model, despite a relatively high R^2 value (Figure 5d). This constant offset is most likely a consequence of processes that are not considered in our simple model. Zr shows a similar pattern but in this case it is over-predicted (Figure 6b). This result is consistent with our observation that the analytical method only partially digests resistate minerals which host Zr. Plotting the misfits spatially shows no spatial bias (e.g. Figure 4b). Inspection of the cross plots for each element shows that the fitted regression lines are generally close to the target 1:1 line.

The RMS and R^2 values for every element are displayed graphically in Figure 7a. For multiple elements, such as V, Rb, U and K, the predictions account for > 70 % of the observed variability (Figure 5). For most elements the R^2 value is > 0.5, which indicates that the model successfully captures the majority of the observed variability.

3.1 Model sensitivity

We quantified the extent to which our model predictions are sensitive to erosional parameters by changing the values in the model and observing resultant model predictions. We find that our model is insensitive to different parameter values. Changing the value of the exponent n between 0–2 in Equation 2 has a very limited effect on the predicted geochemistry and only very weakly affects the model fit (Figure 4c; Figure 7b,c). Similarly, using a different m value of 0.6 also had a small effect on model fit (Figure 7b,c). Assuming a completely homogeneous incision
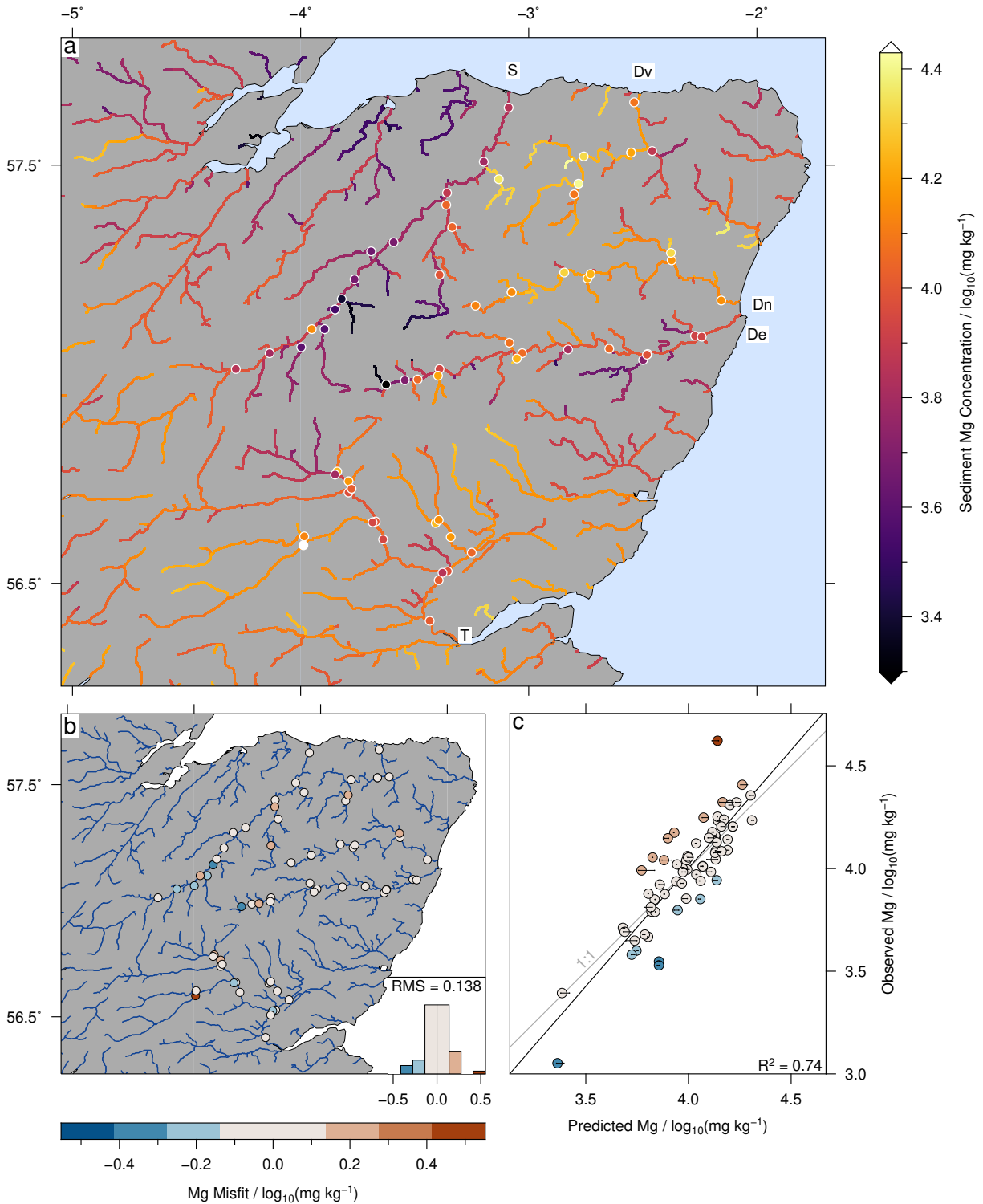
Figure 4: **Comparison of model predictions and observations for Mg**. (a) Coloured circles/curves = observations/predictions of sediment concentrations; note that colours have logarithmic scale. Rivers labelled: S = Spey, Dv = Deveron, Dn = Don, De = Dee, T = Tay. (b) Misfit between observations and predictions at sample sites ($x_{obs} - x_{pred}$); negative (blue) and positive (red) values indicate over- or under-prediction, respectively. Inset histogram shows misfit; bin width is equal to root-mean-square misfit (RMS). (c) Cross plot of observations and predictions. Grey line shows 1:1 relationship. Black line shows linear regression through points, $R^2 = 0.74$. Lines adjacent to points show range of predictions generated by $0.05 \leq n \leq 1.95$ (see Equation 1).
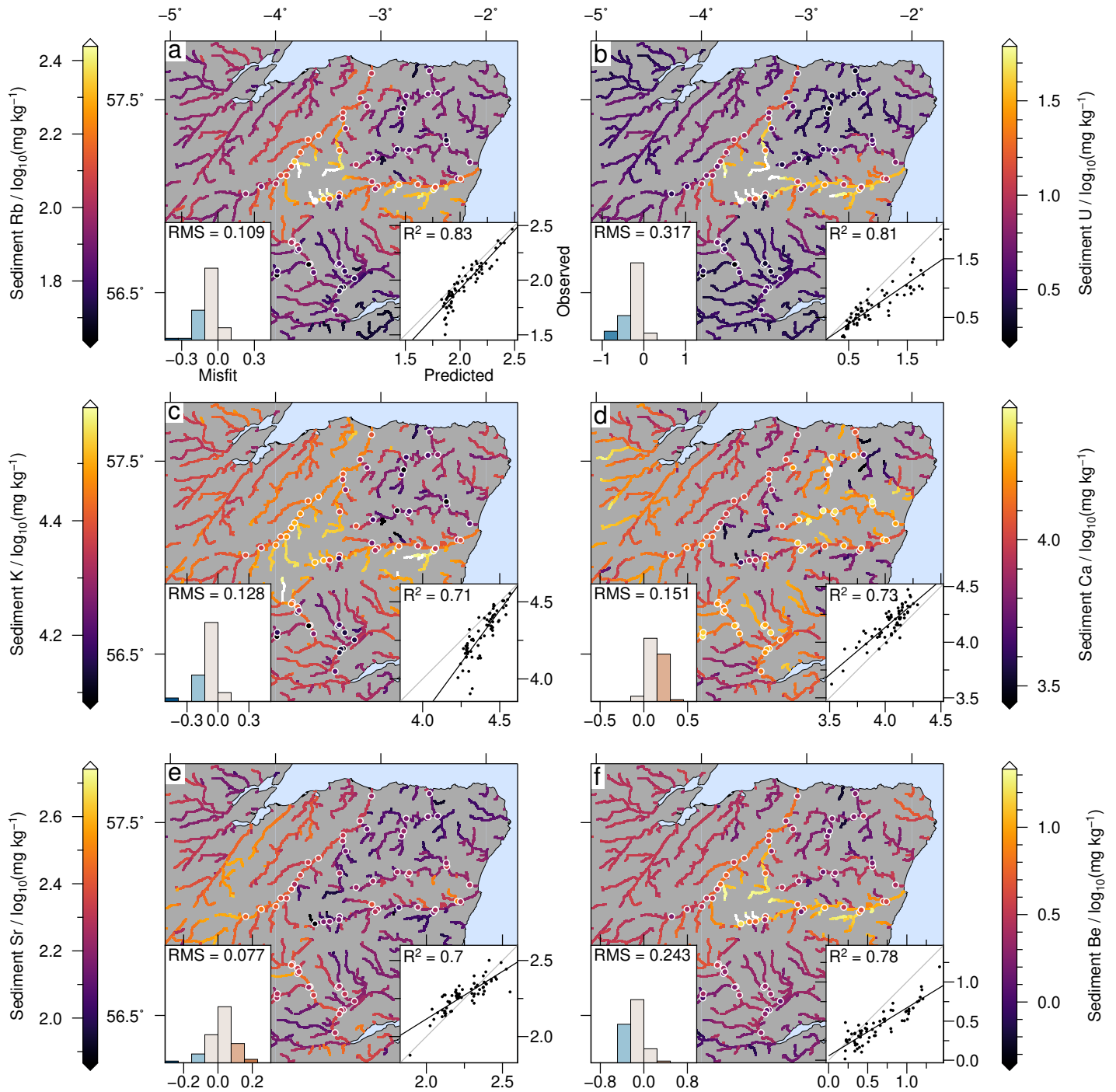
Figure 5: **Comparison of observations and most accurate predictions.** (a) Observed Rubidium concentrations (coloured circles) overlain on model predictions (coloured curves). Note logarithmic colour scale. Right inset shows cross plot of observations and predictions; grey line is 1:1 relationship; black line is linear fit to points; annotation shows R^2 value. Left inset is histogram of misfits; bin width is equal to RMS misfit; blue/red indicate over-/under-prediction. (b) Uranium. (c) Potassium. (d) Calcium. (e) Strontium. (f) Beryllium. Results for elements with less accurate predictions are shown in Figure 6. Results for all other elements are shown in Figure 4 and Supporting Information (Figures S1, S2).
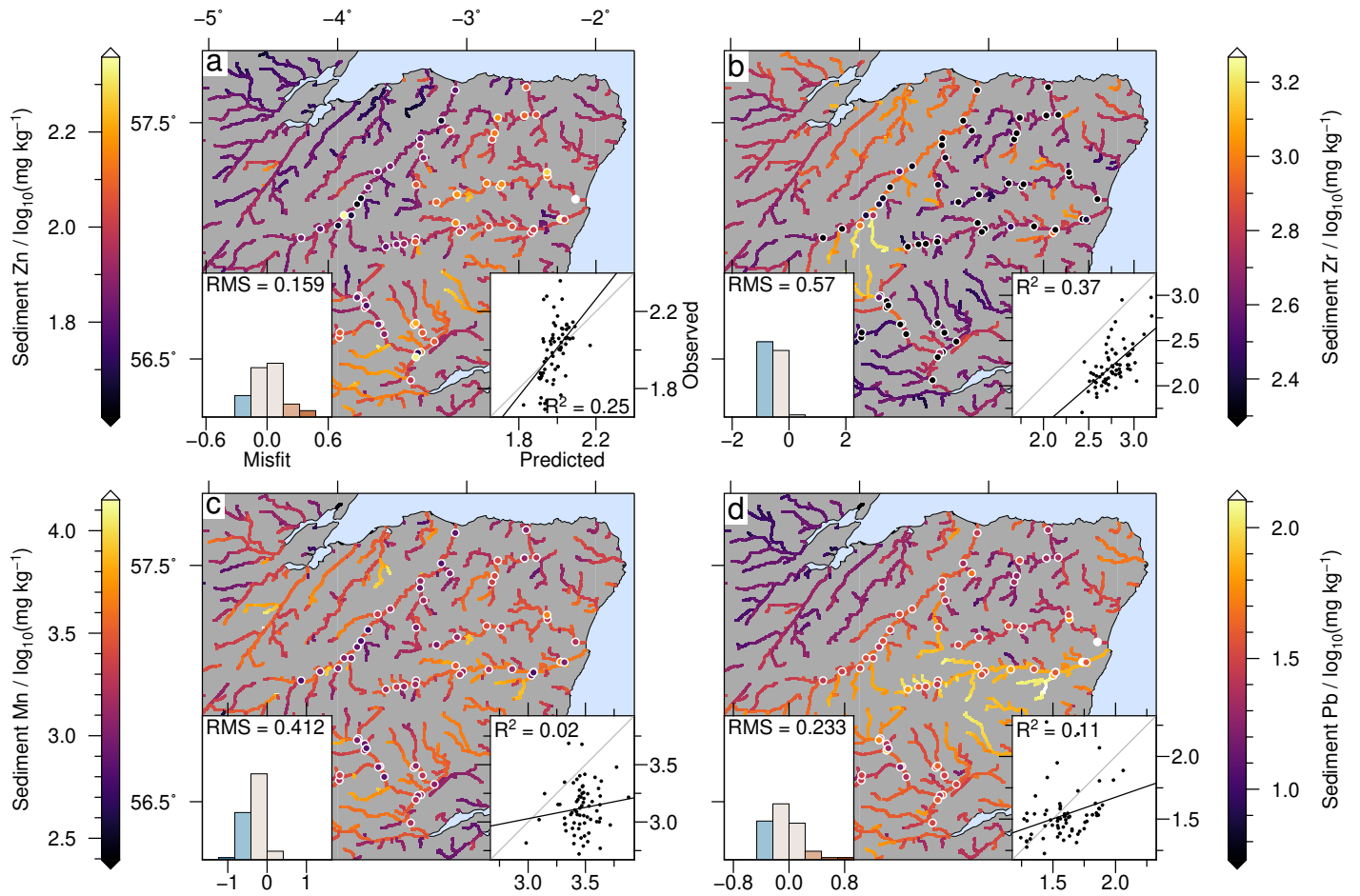
Figure 6: **Comparison of observations and less accurate predictions.** (a) Observed Zinc concentrations (coloured circles) overlain on predictions (coloured curves). Note logarithmic colour scale. Right inset shows cross plot of observations and predictions; grey line is 1:1 relationship; black line is linear fit to points; annotation shows R^2 value. Left inset shows histogram of misfit between observations and predictions; bin width is equal to RMS misfit; blue/red indicate over-/under-prediction. (b) Zirconium. (c) Manganese. (d) Lead. Results for elements with more accurately predicted concentrations are shown in Figure 5. Results for all other elements are shown in Figure 4 and Supporting Information (Figures S1, S2).
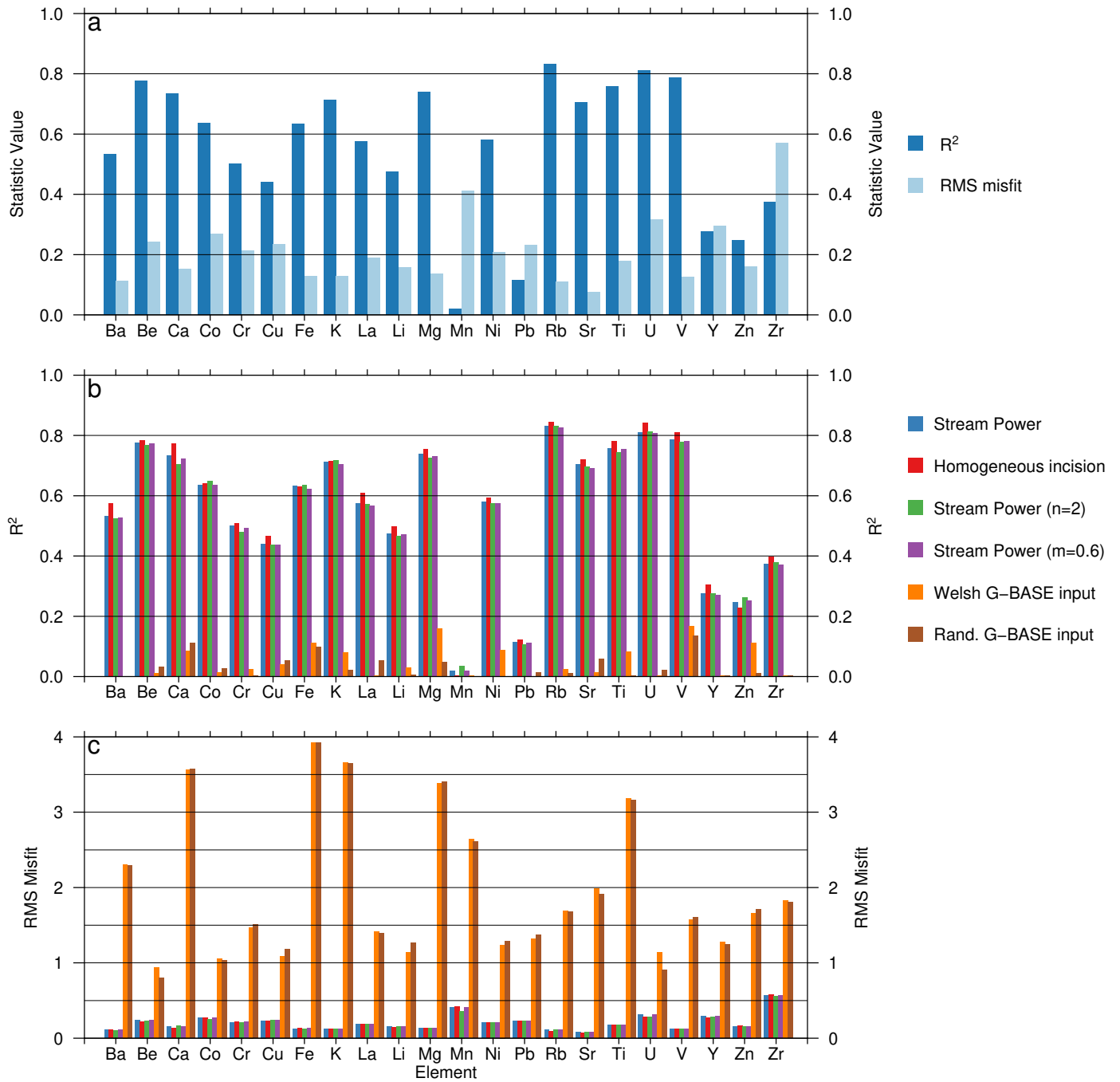
Figure 7: **Evaluation of model predictions.** (a) R^2 and RMS misfit between observed and predicted element concentrations for preferred Stream Power erosional model. (b) R^2 for different models and parameterisations; see key and Supporting Information for visualisation of substrate generated using Welsh G-BASE measurements and a random distribution (Figure S3). (c) RMS misfit for different models/parameterisations.

rate across the studied area has only a minor effect on model fitness (Figure 7b,c).

By contrast, our model is very sensitive to the geochemical input. If the geochemical input is changed, the model predictions are much worse. We explored this sensitivity first by spatially randomising the original G-BASE input prior to interpolation and secondly by using an equally sized rectangle of G-BASE data from an arbitrary chosen part of the UK (Wales). These alternative inputs are shown in Figure 3 of the Supporting Information. Using these different geochemical inputs results in much lower R^2 values for all elements and a significantly higher RMS misfit. Consequently, the success of our model when using the 'true' G-BASE dataset is not simply coincidental and reflects a succesful integration of the upstream geochemistry. This result emphasises that input geochemistry must be known in some detail to make inferences of downstream geochemistry.

4   Discussion

4.1   Predicting sediment geochemistry

The results of the ANOVA indicate that regional variations in river sediment geochemistry dominate over local heterogeneity (Figure 3). Whilst processes such as hydrodynamic sorting and grainsize are generally agreed to affect sediment geochemistry locally, these effects appear to be subordinate to larger regional signals. In this study we account for the effect of sorting using a relatively simplistic process (simply sampling a constant grainsize fraction) but it is likely that more sophisticated measures based on hydrodynamics would better resolve the larger regional signals (e.g. Lupker et al. 2011).

The success of our model indicates that river sediment geochemistry is primarily controlled by conservative mixing of heterogenous source regions. The lack of bias suggests that in-transit modification of sediments by processes such as weathering is a secondary effect, consistent with a recent study of Boron isotopes (Ercolani et al. 2019). An exception to this could be Ca, the concentration of which our model consistently under-predicts. It is possible that cation exchange with the dissolved load could possibly account for this effect, as dissolved Ca is observed to adsorb onto riverine sediments (Cerling et al. 1989). We note that our study area has a relatively temperate climate and does not contain protracted periods of sediment storage in floodplains. Both these factors reduce the possibility of in-transit weathering. The composition of sediments in the Amazon and Ganges rivers, which do have large tropical floodplains, have been interpreted in terms of in-transit sediment modification (Bouchez et al. 2012; Lupker et al. 2012). Nonetheless, in the absence of protracted sediment storage, we suggest that downstream changes in sediment geochemistry should be interpreted primarily as a result of mixing of different source regions not in terms of changing intensity of a particular process. Whilst we consider only elemental geochemistry in this study, similar consideration could perhaps also be applied to sediment hosted isotopic proxies (e.g. Lithium isotopes, $\delta^7 Li$).

4.2   Model sensitivity

Predicted compositions are very sensitive to geochemical input, which suggests that the first order control on river sediment geochemistry is the distribution of source rocks in their catchments.

The dependence on source composition is also a consequence of drainage basins containing fluvial networks that have specific topologies (i.e. geometries and spatial relationships). In contrast, we found that model predictions were insensitive to the fluvial erosional models we tested. We suggest that these results are a consequence of our choice of study area, which probably had a stable Holocene erosional regime. In other regions, where the erosion rates are more spatially variable (e.g. across active faults), we might expect to observe divergence between geochemical predictions from different erosional models. An analogous study to our own, but in a more tectonically active area, would likely allow different erosional models to be discriminated.

4.3   Controls on Cairngorm river sediment composition

A key question is what controls the spatial distribution of elemental concentrations that we have recorded in our river samples. So far we have considered each individual element separately, which effectively results in a 22 dimensional dataset. This high dimensionality makes interpretation challenging. To simplify interpretation, we apply Principal component analysis (PCA) to the higher-order river dataset following a centred log-ratio transformation (Aitchison 1983). PCA is a widely used dimension reduction technique, increasingly applied in sedimentary geochemical analyses (e.g. Vermeesch et al. 2015). PCA works by projecting the raw data onto a smaller number of principal components along which the variance is maximised. Hence by selecting components which contain large amounts of variance, the dimensionality of the dataset is reduced.

For our dataset, 67 % of the total variance is contained on the first principal component (Figure 8d). Inspection of the loadings, i.e. the weightings of the original variables, on the first principal component suggests that it corresponds to a discrimination between mafic and felsic rocks (Figure 8c). Generally, elements with positive loadings are compatible (e.g. Cr, Mg, Ni) whereas elements with negative loadings are incompatible (e.g. Be, K, U). This distribution is confirmed by projecting the G-BASE data onto this component. The resulting map, shown in Figure 8a, clearly defines different geological units (Figure 1b). The felsic intrusions are highlighted in blue, relative to the more mafic rocks shown in red.

This result suggests that the Cairngorms river sediments can be well described simply in terms of having either mafic or felsic source regions. Projecting the predicted and observed sediment compositions onto this principal component confirms this result (Figure 8b). The Spey and Dee rivers are generally more felsic, whereas the Don and Deveron are mafic. The Tay catchment includes both mafic and felsic lithologies, and hence river sediments at its mouth have a more intermediate composition. This analysis emphasises the sensitivity of river sediment compositions to the source region geochemistry. The Don and Dee have contrasting mafic and felsic sediments but for much of their length they share a common watershed and are separated at the mouth by only ~ 4 km.

4.4   Applications and further work

Geochemical surveys such as G-BASE are widely used as baselines for environmental monitoring. Higher order rivers are
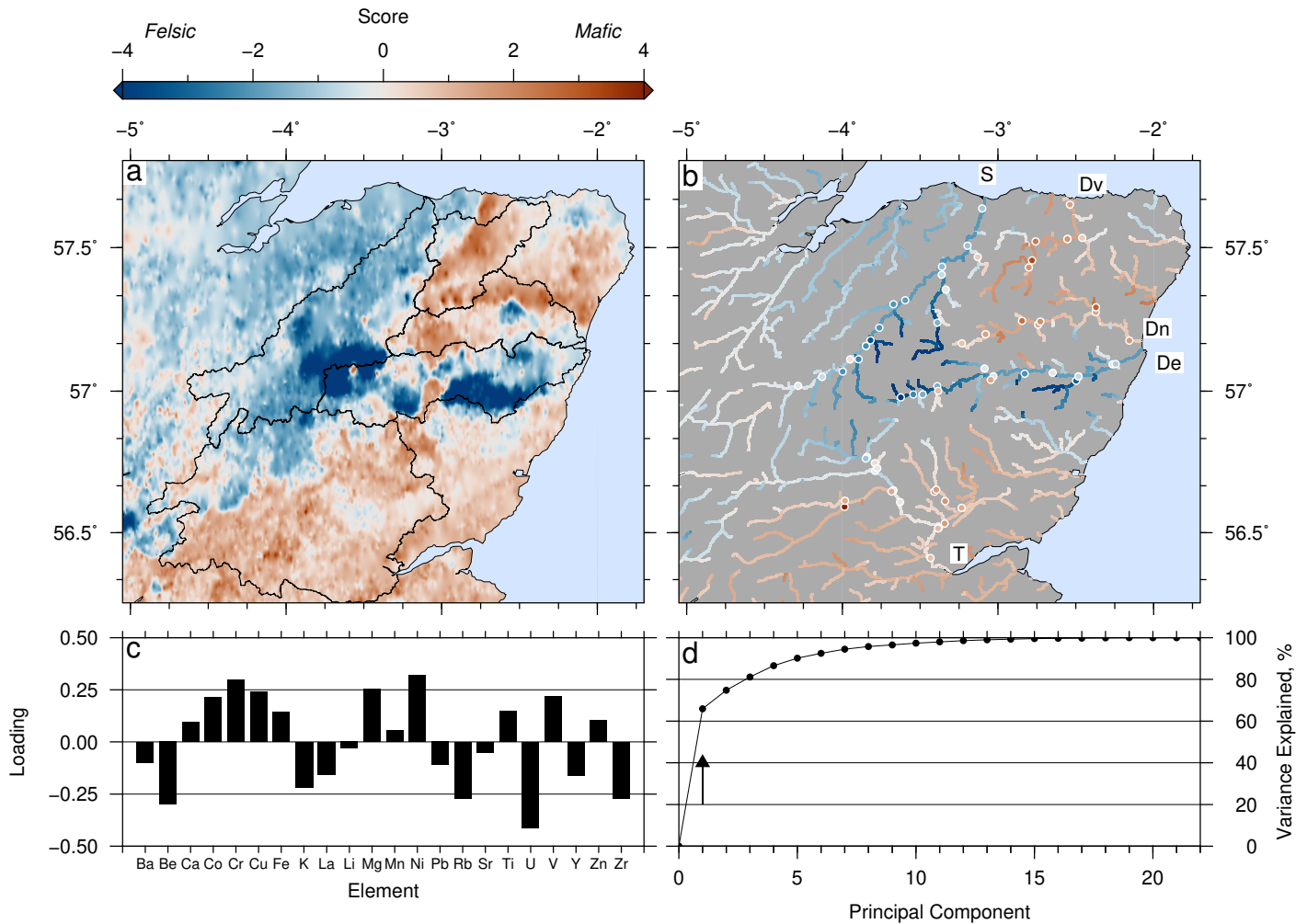
Figure 8: **Principal Component Analysis (PCA) of geochemical data.** PCA is applied to the higher-order river samples following centred log-ratio transformation and the loadings of the principal components were extracted. Observed compositions from the G-BASE data set and model predictions were projected onto these loadings. (a) G-BASE stream sediment data projected onto first principal component and interpolated using minimum curvature spline with tension factor of 0.25. Note the strong relationship to bedrock geology (Figure 1b). (b) Observed and predicted fluvial sediment composition projected onto first principal component. The Spey and Dee carry a more felsic signature whereas the Deveron and Don are more mafic. Rivers labelled: S = Spey, Dv = Deveron, Dn = Don, De = Dee, T = Tay. (c) Loadings on PC1 indicate the geological processes underlying the principal component. Elements with positive loadings are typically associated with mafic igneous rocks whereas negative loadings are associated with felsic rocks. (d) Variance contained on each principal component. Arrow indicates first principal component (displayed here; PC1), which contains 68% (i.e., the majority) of the total variance within the observed geochemical dataset.

rarely included in sampling campaigns (for an exception see Fordyce et al. 2004). Consequently, a generic baseline for environmental monitoring of higher order river sediments is lacking. Extending baseline surveys to include sediments contained in higher-order river sediments, which, as this study shows, integrate geochemistry of their upstream region, is worthwhile. Predictive models such as the one we propose, which utilise survey data as input, could be used to make baseline predictions for higher-order rivers. In places where direct geochemical observations of source regions are sparse, substrate chemistry could be estimated from geological maps and potential field data (e.g. Kirkwood et al. 2016; Wilford et al. 2016)

Our approach of comparing model predictions to real observations allows for critical evaluation of hypotheses about geochemical and geomorphic processes. By evaluating the success of predictions from different erosional models we are implicitly testing hypotheses about which different geomorphic processes are operating. Whilst in our study these different models are relatively equally successful, in alternative regions, an approach akin to one we propose could be used to test different geomorphic assumptions. Furthermore, specific instances where our predictions fail can be used to improve our understanding of geochemical processes. For example, Mn is poorly explained by any model assuming conservative mixing of source regions (Figures 6, 7). We conclude therefore that some other processes, beyond source region mixing, are acting to control the Mn concentration in sediments in our studied rivers.

We have demonstrated that sediment geochemistry can be predicted in rivers from a model that assumes conservative mixing given well constrained source region geochemistry. Here, incision is described by a Stream Power model, although most conservative mixing models appear successful. This predictable behaviour of river sediments suggests that their compositions could be formally inverted to obtain maps of geochemistry in drainage basins. We consider just one time-step in our model, however, it is trivial to extend this model to produce predictions through time. Hence, our approach can be used to forward model, and possibly invert, geochemical signals within the stratigraphic record.

5 Conclusions

We develop a model to predict the geochemical composition of higher order river sediments using erosional models and maps of source region geochemistry. This scheme is tested in a case study of the Cairngorms, UK. Statistical analysis of point measurements gathered across the region show that regional geochemical variability dominates over local heterogeneity. The model accurately predicts observed concentrations of most elements. For our chosen region, the predicted sediment geochemistry is insensitive to the erosional parameters chosen, which is likely due to the specific geomorphic characteristics of our study area. By contrast, we find that sediment geochemistry is highly sensitive to the spatial distribution of the source region geochemistry. River sediment composition is primarily set by conservative mixing of heterogeneous source regions, which can be predicted using simple erosional models. In the Cairngorms, river sediment geochemistry can be described simply in terms of a mixture of mafic and felsic source regions. Our predictive scheme indicates that quantitative modelling, and inversion, of geochemical signals in

the stratigraphic record would likely be successful in revealing the long-term evolution of surface processes.

References

Aitchison, J. (1983). "Principal component analysis of compositional data". *Biometrika* 70.1, pp. 57–65. DOI: 10.1093/biomet/70.1.57.

Barnes, R., C. Lehman, and D. Mulla (2014). "Priority-flood: An optimal depression-filling and watershed-labeling algorithm for digital elevation models". *Computers & Geosciences* 62, pp. 117–127. DOI: 10.1016/j.cageo.2013.04.024.

Blanckenburg, F. von (2005). "The control mechanisms of erosion and weathering at basin scale from cosmogenic nuclides in river sediment". *Earth and Planetary Science Letters* 237.3, pp. 462–479. DOI: 10.1016/j.epsl.2005.06.030.

Blanckenburg, F. von, J. Bouchez, and H. Wittmann (2012). "Earth surface erosion and weathering from the 10Be (meteoric)/9Be ratio". *Earth and Planetary Science Letters* 351-352, pp. 295–305. DOI: 10.1016/j.epsl.2012.07.022.

Bouchez, J., J. Gaillardet, C. France-Lanord, L. Maurice, and P. Dutra-Maia (2011). "Grain size control of river suspended sediment geochemistry: Clues from Amazon River depth profiles". *Geochemistry, Geophysics, Geosystems* 12.3. DOI: 10.1029/2010GC003380.

Bouchez, J., J. Gaillardet, M. Lupker, P. Louvat, C. France-Lanord, L. Maurice, E. Armijos, and J.-S. Moquet (2012). "Floodplains of large rivers: Weathering reactors or simple silos?" *Chemical Geology* 332-333, pp. 166–184. DOI: 10.1016/j.chemgeo.2012.09.032.

Braun, J. and S. D. Willett (2013). "A very efficient O(n), implicit and parallel method to solve the stream power equation governing fluvial incision and landscape evolution". *Geomorphology* 180-181, pp. 170–179. DOI: 10.1016/j.geomorph.2012.10.008.

Caritat, P. d. and M. Cooper (2016). "A continental-scale geochemical atlas for resource exploration and environmental management: the National Geochemical Survey of Australia". *Geochemistry: Exploration, Environment, Analysis* 16.1, pp. 3–13. DOI: 10.1144/geochem2014-322.

Cerling, T. E., B. L. Pederson, and K. L. V. Damm (1989). "Sodium-calcium ion exchange in the weathering of shales: Implications for global weathering budgets". *Geology* 17.6, pp. 552–554. DOI: 10.1130/0091-7613(1989)017<0552:SCIEIT>2.3.CO;2.

Ercolani, C., D. Lemarchand, and A. Dosseto (2019). "Insights on catchment-wide weathering regimes from boron isotopes in riverine material". *Geochimica et Cosmochimica Acta*. DOI: 10.1016/j.gca.2019.07.002.

Farr, T. G., P. A. Rosen, E. Caro, R. Crippen, R. Duren, S. Hensley, M. Kobrick, M. Paller, E. Rodriguez, L. Roth, D. Seal, S. Shaffer, J. Shimada, J. Umland, M. Werner, M. Oskin, D. Burbank, and D. Alsdorf (2007). "The Shuttle Radar Topography Mission". *Reviews of Geophysics* 45.2. DOI: 10.1029/2005RG000183.

Fernandes, V. M., G. G. Roberts, N. White, and A. C. Whittaker (2019). "Continental-Scale Landscape Evolution: A History of North American Topography". *Journal of Geophysical Research: Earth Surface* 124.11, pp. 2689–2722. DOI: 10.1029/2018JF004979.

Fordyce, F. M., B. E. O Dochartaigh, T. R. Lister, R. Cooper, A. Kim, I. Harrison, C. Vane, and S. E. Brown (2004). *Clyde tributaries : report of urban stream sediment and surface water geochemistry for Glasgow*. Internal Report CR/04/037N. Nottingham, UK: British Geological Survey. DOI: http://nora.nerc.ac.uk/id/eprint/18996/10/Erratum.pdf.

Gaillardet, J., B. Dupré, and C. J. Allègre (1999). "Geochemistry of large river suspended sediments: silicate weathering or recycling tracer?" *Geochimica et Cosmochimica Acta* 63.23, pp. 4037–4051. DOI: 10.1016/S0016-7037(99)00307-5.

Garrett, R., C. Reimann, D. Smith, and X. Xie (2008). "From geochemical prospecting to international geochemical mapping: a historical overview". *Geochemistry: Exploration, Environment, Analysis* 8.3-4, pp. 205–217. DOI: 10.1144/1467-7873/08-174.

Garrett, R. G. (1969). "The determination of sampling and analytical errors in exploration geochemistry". *Economic Geology* 64.5, pp. 568–569. DOI: 10.2113/gsecongeo.64.5.568.

Garzanti, E., P. Dinis, P. Vermeesch, S. Andò, A. Hahn, J. Huvi, M. Limonta, M. Padoan, A. Resentini, M. Rittner, and G. Vezzoli (2018). "Dynamic uplift, recycling, and climate control on the petrology of passive-margin sand (Angola)". *Sedimentary Geology*. Analysis of sediment properties 375, pp. 86–104. DOI: 10.1016/j.sedgeo.2017.12.009.

Hobley, D. E. J., J. M. Adams, S. S. Nudurupati, E. W. H. Hutton, N. M. Gasparini, E. Istanbulluoglu, and G. E. Tucker (2017). "Creative computing with Landlab: an open-source toolkit for building, coupling, and exploring two-dimensional numerical models of Earth-surface dynamics". *Earth Surface Dynamics* 5.1, pp. 21–46. DOI: https://doi.org/10.5194/esurf-5-21-2017.

Holbrook, J. and H. Wanas (2014). "A Fulcrum Approach To Assessing Source-To-Sink Mass Balance Using Channel Paleohydrologic Paramaters Derivable From Common Fluvial Data Sets With An Example From the Cretaceous of Egypt". *Journal of Sedimentary Research* 84.5, pp. 349–372. DOI: 10.2110/jsr.2014.29.

Howard, A. D. and G. Kerby (1983). "Channel changes in badlands". *GSA Bulletin* 94.6, pp. 739–752. DOI: 10.1130/0016-7606(1983)94<739:CCIB>2.0.CO;2.

Jager, A. L. d. and J. V. Vogt (2010). "Development and demonstration of a structured hydrological feature coding system for Europe". *Hydrological Sciences Journal* 55.5, pp. 661–675. DOI: 10.1080/02626667.2010.490786.

Johnson, C. C., N. Breward, E. L. Ander, and L. Ault (2005). "G-BASE: baseline geochemical mapping of Great Britain and Northern Ireland". *Geochemistry: Exploration, Environment, Analysis* 5.4, pp. 347–357. DOI: 10.1144/1467-7873/05-070.

Johnson, C. C., E. L. Ander, T. R. Lister, and D. M. A. Flight (2018a). "Chapter 5 - Data Conditioning of Environmental Geochemical Data: Quality Control Procedures Used in the British Geological Survey's Regional Geochemical Mapping Project". In: *Environmental Geochemistry (Second Edition)*. Ed. by B. De Vivo, H. E. Belkin, and A. Lima. 2nd ed. Elsevier, pp. 79–101. DOI: 10.1016/B978-0-444-63763-5.00006-9.

Johnson, C. C., D. M. A. Flight, E. L. Ander, T. R. Lister, N. Breward, F. M. Fordyce, S. E. Nice, and K. V. Knights (2018b). "Chapter 4 - The Collection of Drainage Samples for Environmental Analyses From Active Stream Channels". In: *Environmental Geochemistry (Second Edition)*. Ed. by B. De Vivo, H. E. Belkin, and A. Lima. 2nd ed. Elsevier, pp. 47–77. DOI: 10.1016/B978-0-444-63763-5.00005-7.

Karlstrom, K. E., R. Crow, L. J. Crossey, D. Coblentz, and J. W. V. Wijk (2008). "Model for tectonically driven incision of the younger than 6 Ma Grand Canyon". *Geology* 36.11, pp. 835–838. DOI: 10.1130/G25032A.1.

Kim, S.-M., Y. Choi, H. Yi, and H.-D. Park (2017). "Geostatistical prediction of heavy metal concentrations in stream sediments considering the stream networks". *Environmental Earth Sciences* 76.2, p. 72. DOI: 10.1007/s12665-017-6394-2.

Kirkwood, C., M. Cave, D. Beamish, S. Grebby, and A. Ferreira (2016). "A machine learning approach to geochemical mapping". *Journal of Geochemical Exploration* 167, pp. 49–61. DOI: 10.1016/j.gexplo.2016.05.003.

Lupker, M., C. France-Lanord, V. Galy, J. Lavé, J. Gaillardet, A. P. Gajurel, C. Guilmette, M. Rahman, S. K. Singh, and R. Sinha (2012). "Predominant floodplain over mountain weathering of Himalayan sediments (Ganga basin)". *Geochimica et Cosmochimica Acta* 84, pp. 410–432. DOI: 10.1016/j.gca.2012.02.001.

Lupker, M., C. France-Lanord, and B. Lartiges (2016). "Impact of sediment-seawater cation exchange on Himalayan chemical weathering fluxes". *Earth Surface Dynamics Discussions*, pp. 1–15. DOI: 10.5194/esurf-2016-26.

Lupker, M., C. France-Lanord, J. Lavé, J. Bouchez, V. Galy, F. Métivier, J. Gaillardet, B. Lartiges, and J.-L. Mugnier (2011). "A Rouse-based method to integrate the chemical composition of river sediments: Application to the Ganga basin". *Journal of Geophysical Research: Earth Surface* 116.F4. DOI: 10.1029/2010JF001947.

Paul, J. D., G. G. Roberts, and N. White (2014). "The African landscape through space and time". *Tectonics* 33.6, pp. 898–935. DOI: 10.1002/2013TC003479.

Riebe, C. S., J. W. Kirchner, and R. C. Finkel (2003). "Long-term rates of chemical weathering and physical erosion from cosmogenic nuclides and geochemical mass balance". *Geochimica et Cosmochimica Acta* 67.22, pp. 4411–4427. DOI: 10.1016/S0016-7037(03)00382-X.

Romans, B. W., S. Castelltort, J. A. Covault, A. Fildani, and J. P. Walsh (2016). "Environmental signal propagation in sedimentary systems across timescales". *Earth-Science Reviews*. Source-to-Sink Systems: Sediment & Solute Transfer on the

Earth Surface 153, pp. 7–29. DOI: 10.1016/j.earscirev.2015.07.012.

Rosenbloom, N. A. and R. S. Anderson (1994). "Hillslope and channel evolution in a marine terraced landscape, Santa Cruz, California". *Journal of Geophysical Research: Solid Earth* 99.B7, pp. 14013–14029. DOI: 10.1029/94JB00048.

Salles, T. (2019). "eSCAPE: Regional to Global Scale Landscape Evolution Model v2.0". *Geoscientific Model Development Discussions*, pp. 1–28. DOI: https://doi.org/10.5194/gmd-2019-126.

Salles, T., X. Ding, and G. Brocard (2018). "pyBadlands: A framework to simulate sediment transport, landscape dynamics and basin stratigraphic evolution through space and time". *PLOS ONE* 13.4, e0195557. DOI: 10.1371/journal.pone.0195557.

Sharman, G. R., Z. Sylvester, and J. A. Covault (2019). "Conversion of tectonic and climatic forcings into records of sediment supply and provenance". *Scientific Reports* 9.1, p. 4115. DOI: 10.1038/s41598-019-39754-6.

Smith, D. B., S. M. Smith, and J. D. Horton (2013). "History and evaluation of national-scale geochemical data sets for the United States". *Geoscience Frontiers* 4.2, pp. 167–183. DOI: 10.1016/j.gsf.2012.07.002.

Smith, W. H. F. and P. Wessel (1990). "Gridding with continuous curvature splines in tension". *Geophysics* 55.3, pp. 293–305. DOI: 10.1190/1.1442837.

Stephenson, S. N., G. G. Roberts, M. J. Hoggard, and A. C. Whittaker (2014). "A Cenozoic uplift history of Mexico and its surroundings from longitudinal river profiles". *Geochemistry, Geophysics, Geosystems* 15.12, pp. 4734–4758. DOI: 10.1002/2014GC005425.

Straub, K. M., R. A. Duller, B. Z. Foreman, and E. A. Hajek (2020). "Buffered, Incomplete, and Shredded: The Challenges of Reading an Imperfect Stratigraphic Record". *Reviews of Geophysics*, e2019JF005079. DOI: 10.1029/2019JF005079 @ 10.1002/(ISSN)1944-9208.GRANDCHAL1.

Stucky de Quay, G., G. G. Roberts, D. H. Rood, and V. M. Fernandes (2019). "Holocene uplift and rapid fluvial erosion of Iceland: A record of post-glacial landscape evolution". *Earth and Planetary Science Letters* 505, pp. 118–130. DOI: 10.1016/j.epsl.2018.10.026.

Syvitski, J. P. M. and J. D. Milliman (2007). "Geology, Geography, and Humans Battle for Dominance over the Delivery of Fluvial Sediment to the Coastal Ocean". *The Journal of Geology* 115.1, pp. 1–19. DOI: 10.1086/509246.

Tucker, G. E. and K. X. Whipple (2002). "Topographic outcomes predicted by stream erosion models: Sensitivity analysis and intermodel comparison". *Journal of Geophysical Research: Solid Earth* 107.B9, ETG 1–1–ETG 1–16. DOI: 10.1029/2001JB000162.

Van Rossum, G. and F. L. Drake (2009). *Python 3 Reference Manual*. Scotts Valley, CA: CreateSpace.

Vermeesch, P. and E. Garzanti (2015). "Making geological sense of 'Big Data' in sedimentary provenance analysis". *Chemical Geology* 409, pp. 20–27. DOI: 10.1016/j.chemgeo.2015.05.004.

Weltje, G. J. (2012). "Quantitative models of sediment generation and provenance: State of the art and future developments". *Sedimentary Geology*. Actualistic Models of Sediment Generation 280, pp. 4–20. DOI: 10.1016/j.sedgeo.2012.03.010.

Wessel, P., W. H. F. Smith, R. Scharroo, J. Luis, and F. Wobbe (2013). "Generic Mapping Tools: Improved Version Released". *Eos, Transactions American Geophysical Union* 94.45, pp. 409–410. DOI: 10.1002/2013EO450001.

Whipple, K. X. and G. E. Tucker (2002). "Implications of sediment-flux-dependent river incision models for landscape evolution". *Journal of Geophysical Research: Solid Earth* 107.B2, ETG 3–1–ETG 3–20. DOI: 10.1029/2000JB000044.

Wilford, J., P. de Caritat, and E. Bui (2016). "Predictive geochemical mapping using environmental correlation". *Applied Geochemistry* 66, pp. 275–288. DOI: 10.1016/j.apgeochem.2015.08.012.

Supporting Information

The supporting information contains three supplementary figures showing the results of the predictive scheme described in the main document and a video showing the higher-order river sediment sampling procedure. Figures S1 and S2 contain the results for all elements not displayed in the main manuscript (Figures 4, 5 and 6). The interpretation of these figures is the same as described in the main document. Figure S3 indicates the resulting predictions if the geochemical input to the model is changed. Here this is demonstrated firstly by using a section of the G-BASE dataset but taken from elsewhere in the UK (arbitrarily, Wales) and secondly by spatially randomising the G-BASE input from the study region before interpolation. Neither approach gives good results suggesting that the success of our model when utilising the G-BASE dataset is not simply coincidental. This results further emphasises the sensitivity of downstream geochemistry to the specific upstream geochemical distribution.

The supporting video showing the sampling procedure can be found at github.com/AlexLipp/predict-river-chem.
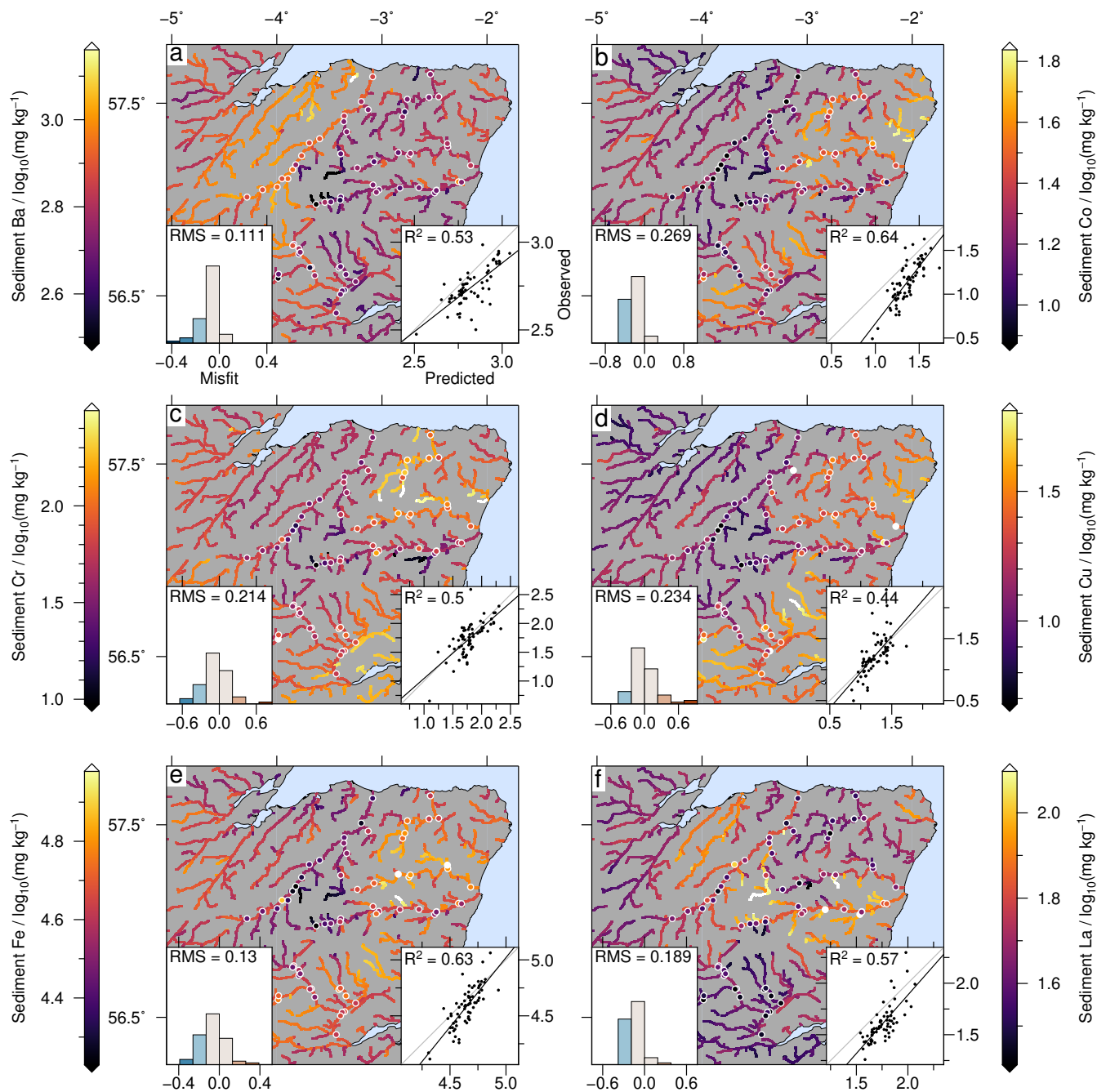
Supplementary Figure 1: Results for other elements modelled by our approach. This figure is interpreted in the same way as Figures 5 and 6 in the main document
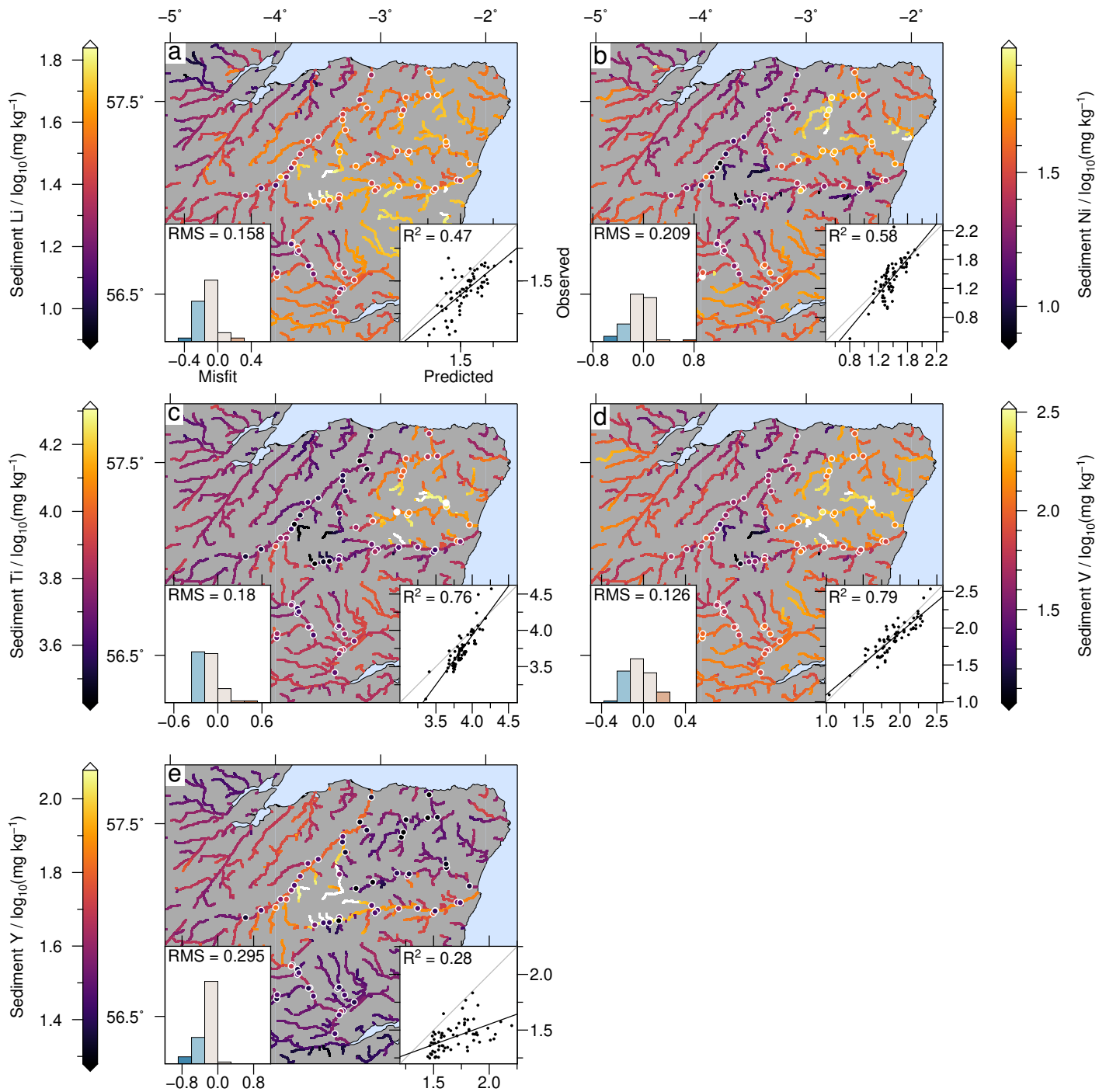
Supplementary Figure 2: Results for other elements modelled by our approach. This figure is interpreted in the same way as Figures 5 and 6 in the main document
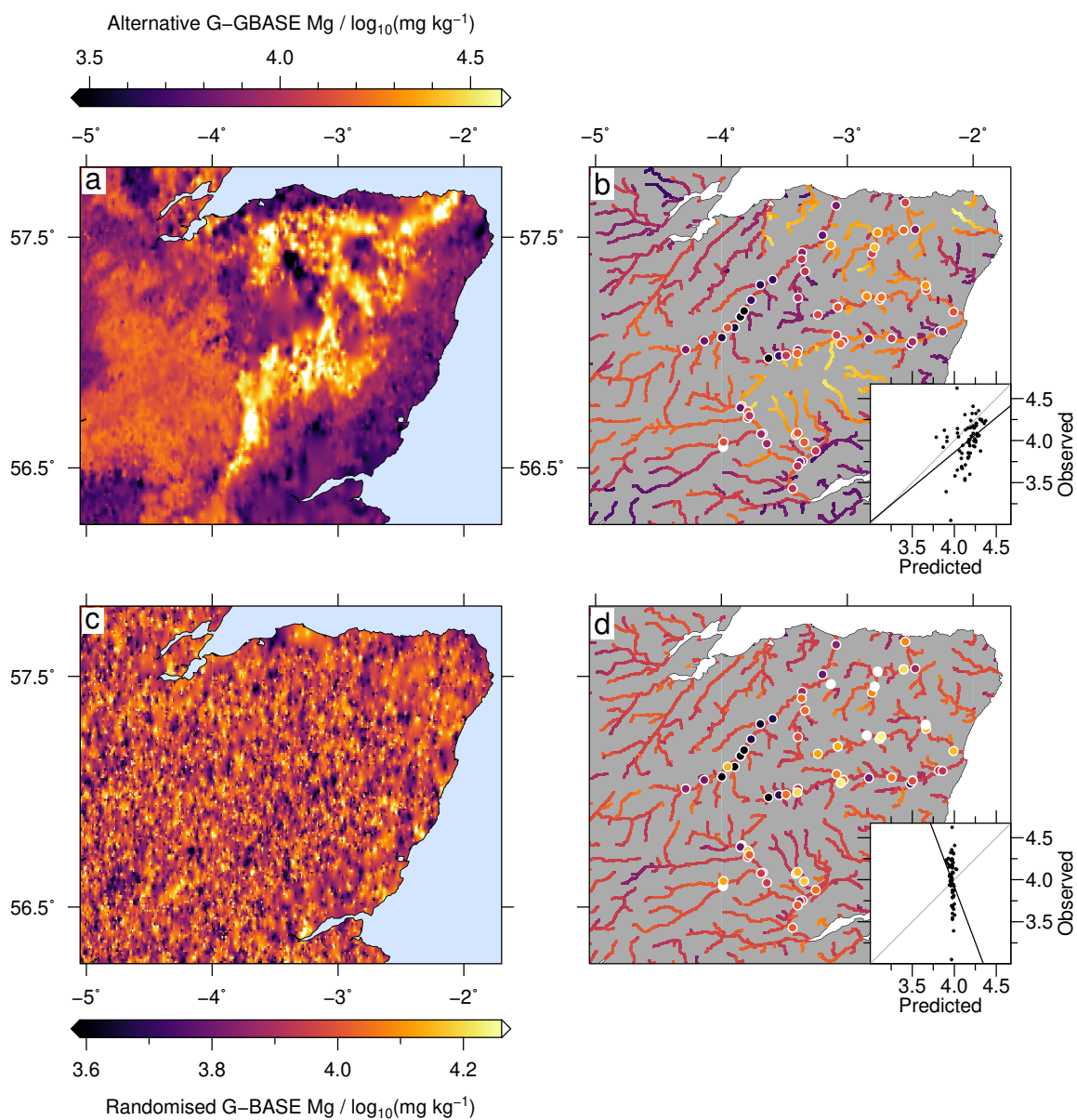
Supplementary Figure 3: Results for Mg when different geochemical inputs are made. a) Interpolated G-BASE grid taken from elsewhere in UK, here Wales/Herefordshire. b) Results of using this input compared to observed data. c) Interpolated grid created when randomising the Cairngorms GBASE samples. d) Results of using this input compared to observed data.